RESEARCH ARTICLE

Magnetic-Thermal-Flow Field Coupling Simulation of Oil-Immersed Transformer

XINYAN FENG[1], DA ZHANG[1], TINGZHI ZHAO[1], HAN LIU[1], YOUFEI SUN[1],
HAOXIN GUO [2], AND DONGXIN HE [2]
[1]State Grid Shandong Electric Extrahigh Voltage Company, Jinan 250021, China
[2]Shandong Provincial Key Laboratory of UHV Transmission Technology and Equipment, School of Electrical Engineering, Shandong University, Jinan 250061, China

Corresponding author: Dongxin He (hdx@sdu.edu.cn)

ABSTRACT Accurately understanding the temperature field distribution and hot-spot temperature of oil-immersed transformers is of great significance for ensuring the safe and stable operation of the transformer. A magnetic-thermal-flow coupling simulation model for oil-immersed transformer is established in this paper. In order to better simulate the heat dissipation process of the transformer, the winding uses a pie shaped structure with interval arrangement instead of the traditional cylindrical structure. The losses of iron core and winding are calculated through magnetic field simulation. Then, the losses are used as heat source for coupling simulation of thermal field and laminar flow to obtain the oil flow distribution, 3-D temperature field distribution, and temperature and location distribution of hot-spot. Finally, coupling simulations are conducted under different load currents to analyze the impact of load currents on the temperature and location of transformer hotspots. The simulation results show that as the current increases, the hot-spot temperature increases. When the load current changes, the hot-spot fluctuates within the range of 85% -90% of the total height of the low-voltage winding, providing a methodological basis for the maintenance of transformers and monitoring of hot-spot temperatures.

INDEX TERMS Transformer, magnetic-thermal-flow field, temperature field, hot-spot temperature.

I. INTRODUCTION

The main function of transformers in the power system is to transform voltage to facilitate the transmission of electrical energy, which plays a crucial role in ensuring the safe and stable operation of the entire power system. The insulation structure of oil-immersed transformers is oil-paper insulation, which is a combination of transformer oil and insulation paper. The gaps in the transformer are filled with transformer oil. High temperature can lead to the aging and degradation of insulation materials inside trans-formers, increasing the risk of electrical faults, and can also cause the decomposition of transformer oil, producing sediment and gases, which may reduce the insulation performance and cooling effect

The associate editor coordinating the review of this manuscript and approving it for publication was Norhafiz Azis.

of the transformer oil [1], [2]. Therefore, temperature is a very important operating control parameter for oil-immersed transformers. Monitoring the hot spot temperature of the transformer, studying the causes and diagnostic methods of abnormal hot spot temperature are of great significance.

The recent research on transformer hot spot temperature is mainly divided into two types: direct measurement method and indirect measurement method. The direct measurement method directly measures the temperature of a hot spot by embedding sensors inside the transformer. This method has high measurement accuracy and can achieve real-time monitoring. Moreover, the embedded sensors are not affected by ex-ternal environmental factors, making the measurement more stable [3], [4]. Nicola et al. designed a monitoring system based on LabVIEW that uses fiber optic sensors to measure the hot spot temperature of transformer windings,

which can display the online evolution of temperature [4]. Jiang et al. designed a thermal sensor based on fiber Bragg grating for the online temperature measurement system in oil-immersed trans-formers, and the measurable range is 30 °C to 150 °C, with resolution of 1 °C [5]. However, the direct measurement method can destroy the structure of the trans-former, and has high costs, complex installation, and high requirements for equipment and personal safety. The indirect measurement method is to indirectly calculate the temperature of the transformer hot spot through calculation formulas or building simulation models, mainly including empirical formula method, thermal circuit model method and numerical simulation method [6], [7]. The indirect measurement method ensures the integrity of the transformer structure, but its measurement accuracy is limited by the quality of the input data and the calculation model. If the input data or calculation model is not accurate enough, the measurement accuracy will be affected [8]. Meanwhile, both empirical formula method and thermal circuit model method cannot reflect the internal temperature field distribution of transformers, and the influence of transformer winding structure and heat dissipation medium is not considered. Therefore, scholars begin to study numerical simulation methods based on muti-physics field coupling. Liu et al. coupled heat transfer field and fluid heat field to simulate the temperature filed distribution [9]. Das and Chatterjee et al. simulated the flow rate distribution and analyzed the hot-spot in an oil-filled disc type winding of transformer using COMSOL based 2D and 3D model [10]. Mafra et al. calculated the hottest-spot transformer temperature under free convection through the resolution of the heat conduction equation in three dimensions using COMSOL Multiphysics [11]. Khandan et al. used a free open-source computational fluid dynamics fluid dynamics solver Open-FOAM to simulate the temperature distribution and fluid flow of an oil cooled winding of a power transformer [12]. Guo et al. applied ICEM CFD software to establish a simplified model of a discrete transformer and used the Boussinesq model in Fluent to simulate the thermal and oil flow fields inside the transformer, obtaining the specific temperature and hot spot location of the transformer [13]. The above are all about the coupling simulation of thermal field and flow field. The heat source is mostly obtained through theoretical calculation or experiment. Recently, some scholars conducted magnetic-heat-flow coupling simulation to obtain losses as heat source. Jing et al. proposed an electromagnetic-fluid-thermal coupling method to calculate the hot-spot temperature rise of the transformer [14]. Li et al. also proposed an electromagnetic-fluid-thermal coupled approach, which obtained the losses through 3D FEM calculations and calculated the oil flow distribution through CFD [15]. Li et al. established a three-dimensional magnetic-heat-flow multi-physical field simulation model, and calculated the hot spot temperature of transformer under different ambient temperature and load coefficient [16].

As can be seen from the above, the numerical simulation of transformers focuses on the coupling of multiple physical fields, especially the coupling of heat transfer and fluid fields. The magnetic-thermal-fluid coupling simulation focuses on the analysis of temperature field and oil flow field, with less analysis of hot-spot temperature and position, and less research on the influence of load current on hot-spot temperature and position. Moreover, in order to simplify the model, most people choose to simplify the 3D model to 2D and simplify the winding to a cylinder, which can result in inaccurate simulation results. This paper proposes a magnetic-thermal-flow coupling simulation method based on finite element analysis. When modeling, the winding uses a pie shaped structure with interval arrangement instead of the traditional cylindrical structure, which can better simulate the heat dissipation process of the transformer and improve the accuracy of simulation results. The losses of the iron core and coil are calculated through magnetic field simulation. Then the losses are used as a heat source for thermal-flow coupling simulation to obtain the oil flow distribution, three-dimensional temperature field distribution, and hot spot temperature and location distribution. Finally, simulations are conducted under different load currents to analyze the impact of load currents on the temperature and location of transformer hotspots, providing a methodological basis for the maintenance of transformers and monitoring of hot-spot temperatures.

II. PRINCIPLE OF TRANSFORMER TEMPERATURE RISE

During the working process of an oil-immersed transformer, the losses generated by the iron core and winding will be converted into heat, causing the temperature rise of the transformer [17]. The loss generated by the iron core is the magnetic loss caused by the alternating magnetization of the iron core, which mainly includes hysteresis loss and eddy current loss. Hysteresis loss is the energy loss caused by magnetic hysteresis during the process of repeated magnetization of an iron core. Eddy current loss is the resistance loss generated by the eddy current inside the iron core under the action of an alternating magnetic field. The loss generated by the winding mainly includes resistance loss and inductive loss. Resistance loss is caused by the limited resistance of the winding, which results in resistance loss when current passes through the winding. Inductive loss is caused by the constant variation of current in the winding with voltage, resulting in energy loss caused by alternating inductance. Therefore, in order to obtain the temperature field distribution inside the transformer during operation, it is necessary to first calculate the losses of the iron core and winding.

For iron core, empirical Steinmetz and Bertotti models can be used to calculate the total losses caused by hysteresis loss and eddy current loss. The Steinmetz model mainly considers the relationship between core loss density and material properties, magnetization frequency, and magnetic flux density amplitude. The Steinmetz equation is given as follows [18]

$$W_i = K_h f^\alpha B_m^\beta \tag{1}$$

where W_i is the core loss density, K_h, α and β are the loss coefficient, f is the frequency of magnetic flux density

variation, B_m is the largest magnetic flux density. The magnetic flux density is mainly decided by the magnetic iron, and the equation shows that the iron core loss varies linearly with the frequency.

For winding, ignoring the influence of the leakage flux and only considering resistance loss, the formula for calculating the resistance loss density of the winding is as follows

$$W_c = \frac{1}{T_w} \int_{t_{end}-t}^{t_{end}} J \cdot E dt \qquad (2)$$

where W_c is the winding loss density, T_w is the period, J is the volume current density, E is the electric field intensity, and t is the time value.

When only considering resistance loss, the winding loss of transformer can be directly calculated by the following formula

$$P_c = I^2 \cdot R \qquad (3)$$

where P_c is the winding loss, I is the rated current of the transformer, and R is the resistance of the transformer winding.

After obtaining the losses of the transformer iron core and winding from the above calculation formula, coupling the losses data as a heat source with the laminar flow interface can calculate the temperature field distribution of the transformer. The heat transfer during the coupling process of transformer heat transfer and laminar flow is shown in Figure 1. The heat generated by the losses of the iron core and winding is first transferred to the transformer oil through thermal conduction. An increase in the temperature of the transformer oil leads to a decrease in density. The high temperature transformer oil floats up under the action of gravity, transferring heat to the oil tank wall of the transformer. The oil tank wall comes into contact with the external air to transfer heat. After cooling, the transformer oil sinks to the lower part, completing the cooling and heat dissipation of the transformer [19].
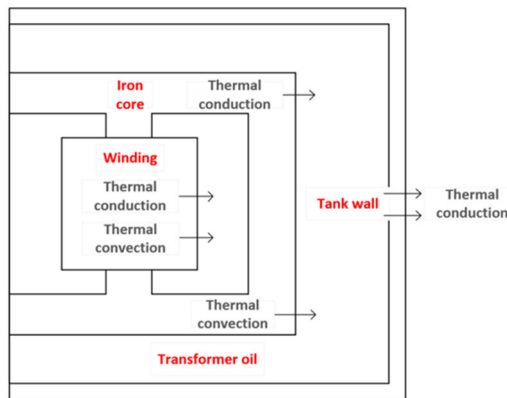

FIGURE 1. Schematic diagram of internal heat transfer in transformer.

III. MULTI-PHYSICS FIELD SIMULATION THEORY
A. MAGNETIC FIELD
The temperature rise of the transformer comes from the losses of the iron core and winding. To accurately obtain the losses of the iron core and winding, it is necessary to conduct magnetic field simulation on the oil-immersed transformer. For the magnetic field of the transformer, solving the Maxwell equations under established boundary conditions can obtain the relationship between the stable magnetic field H formed by the current density J in the coil in the medium and the magnetic induction intensity B. The expression is as follows

$$\nabla \times H = J \qquad (4)$$
$$\nabla \bullet B = 0 \qquad (5)$$
$$B = \mu H \qquad (6)$$

The iron core of the transformer is composed of multiple layers of thin silicon steel sheets, and its magnetization model adopts the relative permeability model. The formula is as follows

$$B = \mu_0 \mu_r H \qquad (7)$$

where B is the magnetic induction intensity, H is the magnetic field intensity, μ_0 is the vacuum magnetic permeability, and μ_r is the magnetic permeability of the iron core.

Materials with current density proportional to electric field can be described using the constitutive equation of Ohm's law, which is as follows [20]

$$J = \sigma E \qquad (8)$$

where σ is the conductivity, E is the electric field intensity. Due to the passivity of magnetic field, the passive field can be represented as the curl of another vector based on vector analysis. Usually, the vector magnetic vector potential A is introduced, and the expression is as follows

$$B = \nabla \times A \qquad (9)$$

The B-H curve of the iron core reflects the magnetization characteristics of the iron core, and the B-H curve of the iron core is shown in Figure 2.
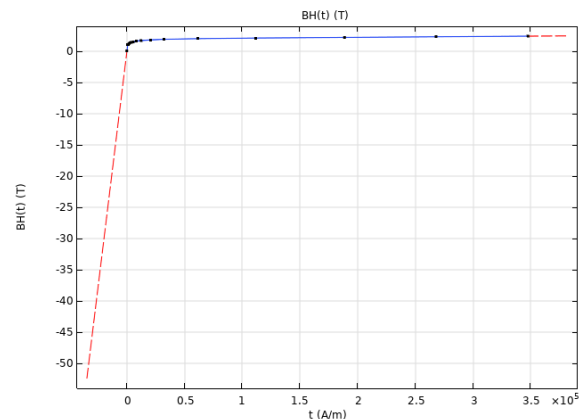

FIGURE 2. B-H curve of iron core.

B. THERMAL-LAMINAR FLOW COUPLING FIELD

There are three ways of thermal transmission: thermal conduction, thermal convection, and thermal radiation. In the simulation of transformer temperature field, the in-fluence of thermal radiation is ignored, and only thermal conduction and convection are considered. Thermal conduction is generated by the transfer of energy between adjacent particles. The energy transfer in thermal conduction is related to the thermal conductivity and temperature difference of the material, and is proportional to the temperature gradient. Its heat flux is calculated by the following equation

$$q = -k \frac{dT}{dx} \tag{10}$$

where q is the heat flux, k is the thermal conductivity, T is the temperature, and x is the coordinate on the thermal conductivity surface.

Thermal convection refers to heat transfer occurring within a fluid flowing at a certain velocity, where energy is transferred through the flow. The heat flux is calculated by the following formula [21]

$$q = h(T - T_0) \tag{11}$$

where h is convective heat transfer coefficient, T is the temperature on the surface of an object, and T_0 is the temperature of fluid.

The transformer simulated in this paper adopts the oil-natural air-natural (ONAN) cooling method. The working principle of an ONAN transformer is to utilize the natural convection of transformer oil to drive the heat generated by the transformer to the surface of the oil tank wall. Then, under the action of air convection and air heat conduction, the heat is dissipated. Therefore, coupling simulation of thermal and fluid fields is required. Transformer oil is a fluid with a low flow velocity and low Reynolds number, which can be regarded as laminar flow. The motion and heat transfer of fluid can be expressed by the balance of mass, momentum, and total energy, which is described by the continuity equation, Navier-Stokes equation, and total energy equation, as follows [22]

$$\frac{\partial \rho}{\partial t} + \nabla \bullet (\rho u) = 0 \tag{12}$$

$$\rho \frac{\partial u}{\partial t} + \rho u \cdot \nabla u = -\nabla p + \nabla \cdot \tau + F + \rho g \tag{13}$$

$$\rho C_P \frac{\partial T}{\partial t} + \rho C_P u \bullet \nabla T = \nabla \bullet (k \nabla T)$$
$$+ \nabla \bullet (-pu + \tau \cdot u) + Q \tag{14}$$

where ρ is the temperature-dependent density of the transformer oil, u is the fluid velocity, p is the fluid pressure, τ is the viscous stress tensor, F is the volume force, g is the gravitational acceleration, C_P is the specific heat capacity, k is the thermal conductivity, T is the temperature, Q is the heat flux, and ∇ is a Hamiltonian operator.

IV. FINITE ELEMENT ANALYSIS OF MULTI-PHYSICS FIELD SIMULATION

A. MODELING

To reduce simulation time and improve model convergence, the transformer model is reasonably simplified, as shown in Figure 3.
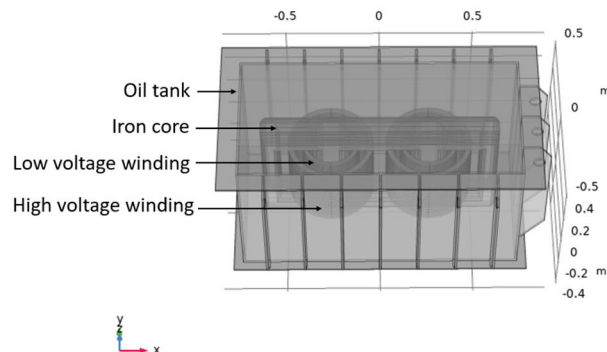

FIGURE 3. The curve of physical parameters of transformer oil changing with temperature.

The simplified model of a transformer mainly consists of the oil tank shell, trans-former oil, iron core, and winding. The volume of the oil tank shell is 1.48 m × 0.732 m × 0.83 m. The material of the oil tank shell is structural steel, and the inside of the oil tank is filled with transformer oil. An iron core and winding are placed in the middle of the oil tank. The material of the iron core is soft iron, and the material of the winding is copper. The winding model is a pie shaped structure with interval arrangement, divided into low-voltage winding and high-voltage winding. The inner diameter of the low-voltage winding is 0.13 m, and the outer diameter is 0.151 m. The inner diameter of the high-voltage winding is 0.199 m, and the outer diameter is 0.227 m. The physical parameters of the solid components inside the transformer are shown in Table 1.

TABLE 1. Physical parameters of solid components of transformers.

component	density/ (KG·M^{-3})	Thermal conductivity/ (W·m^{-1}·K^{-1})	Heat capacity at constant pressure/ (J·kg-1·K-1)
Iron core	7650	191	0.52
winding	8960	400	385
tanker	7850	44.5	475

The physical parameters of transformer oil are affected by temperature. The variation curves of its dynamic viscosity (eta), constant pressure heat capacity (Cp), density (rho), and thermal conductivity (k) with temperature are shown in Figure 4.

Finite element numerical analysis requires mesh partitioning. The density of mesh partitioning determines the calculation accuracy and simulation time. Due to the complexity of the transformer model, multiple mesh partitioning
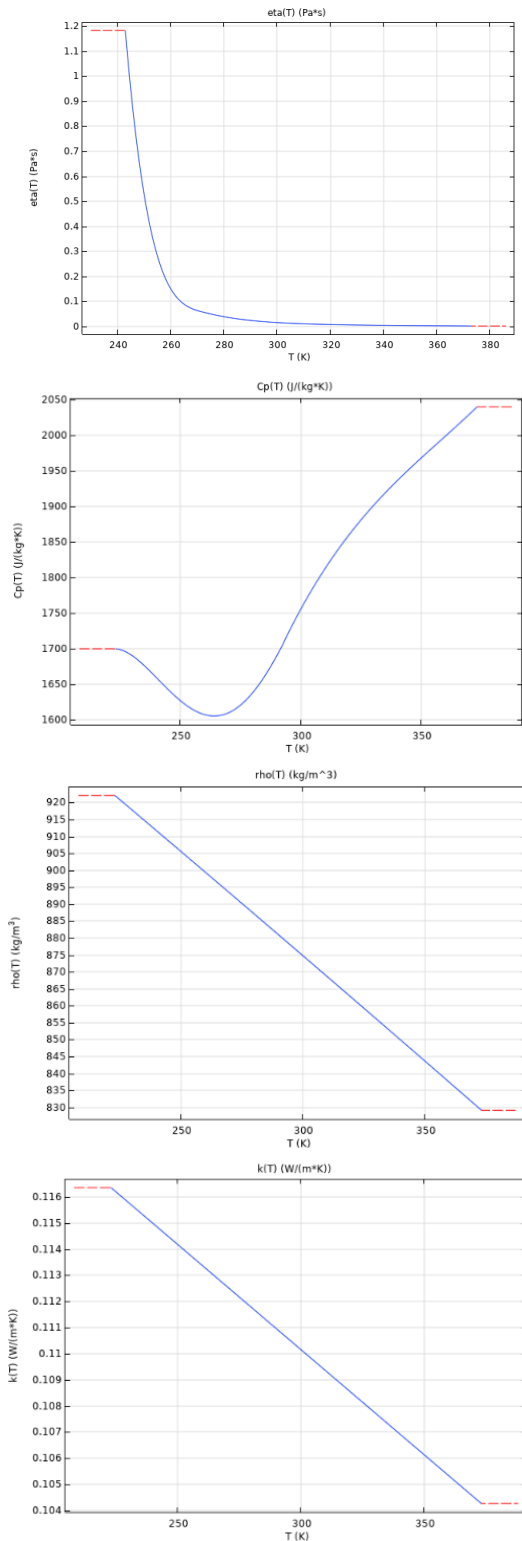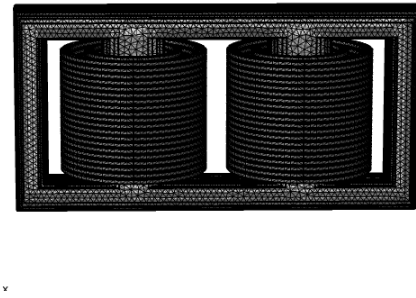
FIGURE 5. The diagram of transformer mesh division.

finely divided than the rest. This simulation has a total of 1213871 grid cells, with an average cell mass of 0.6095. The mesh division of the iron core and winding is shown in Figure 5.

B. MAGNETIC FIELD

When conducting three-dimensional magnetic field simulation on the transformer, current excitation needs to be applied to both low-voltage winding and high-voltage winding. Firstly, apply a 180 A current to the low-voltage winding and 70 A current to the high-voltage. Through geometric analysis of the coil, the geometric dimensions (length, cross-section) of the coil wire can be calculated to determine the resistance of the coil and the direction of the current. The low-voltage coil resistance is 0.103 Ω, and the high-voltage coil resistance is 0.408 Ω. Then, the magnetic flux density mode distribution of the iron core and winding can be obtained through frequency domain calculation. The boundary condition of magnetic field simulation is magnetic insulation, and the initial value of the magnetic vector potential is (0,0,0) Wb/m. The frequency is set to 50 Hz, and the magnetic flux density mode distribution of the iron core and winding calculated in the frequency domain is shown in Figure 6.
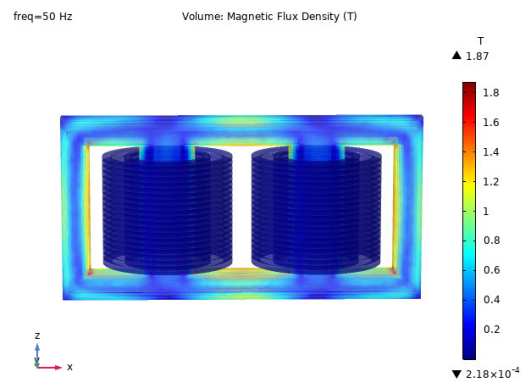

FIGURE 6. Three-dimensional distribution diagram of magnetic flux density mode for iron core and coil.

FIGURE 4. Geometric model of transformer.

method is used for mesh partitioning. To reduce simulation time while meeting the requirements of computational accuracy, a method of mesh partitioning with different densities in different regions is adopted. For the oil-immersed transformer model, the mesh of the iron core and winding is more

As shown in Fig. 6, during the operation process of the transformer, the magnetic field presents a symmetrical distribution from top to bottom. The magnetic flux density at the four sharp corners of the outer window of the iron core is

relatively small, while the magnetic flux density at the corners of the inner window of the iron core is larger. There is a saturation phenomenon of magnetic flux density at the connection between the core column and the upper and lower yokes, with a maximum magnetic flux density of 1.87 T. The saturation of magnetic flux density at these connections is prone to local overheating. Due to the influence of transformer oil medium in the winding, the magnetic flux density of the winding is smaller and the overall distribution is relatively uniform [23].

The finite element simulation software provides a loss calculation subfunction to calculate losses. The empirical Steinmetz equation is used to calculate iron core loss, as shown in formula (1). The proportionality constant K_h is 1000 W/m^3, the exponent α for frequency is 1, and the exponent β for magnetic flux density is 1.5. The resistance loss option in the loss calculation subfunction (based on Ohm's law) is used to calculate winding loss. The volume loss density distribution of the iron core through loss calculation is shown in Figure 7.
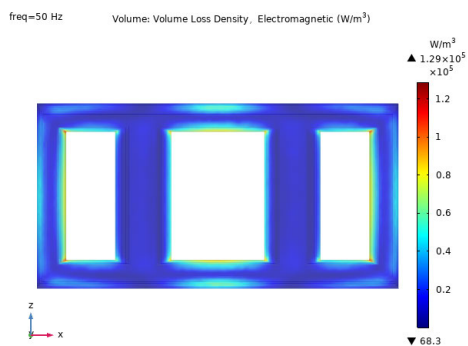

FIGURE 7. The volume loss density distribution diagram of the iron core.

As shown in Figure 7, it can be seen that the loss density at the connection of the iron core column is relatively high, and the loss density at the end corners is relatively low. This distribution is basically consistent with the magnetic flux density mode distribution of the iron core, with a maximum loss density of 1.29×10^5 W/m^3. According to formula (1), the theoretical value of the maximum loss density of the iron core is calculated as 1.279×10^5 W/m^3. The simulation result of 1.29×10^5 W/m^3 is very close to the theoretical value. The total losses calculated through volume integration are shown in Table 2. According to formula (3), the theoretical values of the losses of the low-voltage winding and high-voltage winding are 3337.2 W and 1999.2 W. The simulation values of the losses of the low-voltage winding and high-voltage winding are 3322.2 W and 1964.3 W, which are very close to the theoretical values, proving the validity of the simulation model.

TABLE 2. Iron core and winding losses.

Heat source	Iron core	Low-voltage winding	High-voltage winding
Total losses/W	1124.3	3322.2	1964.3

C. COUPLING OF THERMAL AND LAMINAR FLOW FIELD

According to the principle of transformer temperature rise, temperature distribution simulation requires coupling of thermal field and laminar flow field. The boundary conditions of the thermal field can be seen in table 3. The heat transfer between the oil tank wall and the air belongs to convective heat transfer [24]. The heat transfer coefficient is 10 W/(m^2·K). The iron core and winding losses calculated by the magnetic field are set as heat sources in the solid and fluid heat transfer module. The initial temperature of the transformer and the external environ-mental temperature are both set as 20 °C. The transformer oil domain is set as a laminar flow domain, and the boundary condition is set as no slip. The flow field calculation includes gravity, and the gravitational acceleration along the negative z-axis is 9.8 m/s^2. To enable the model to converge faster, the initial speed of transformer oil is set to 0.01 m/s, with the direction along the positive z-axis [25]. A non-isothermal flow multi-physical field interface is selected to couple the laminar flow field and the solid and fluid heat transfer field. Then, steady-state calculations are used to obtain the velocity and temperature field distribution of the transformer under thermal equilibrium state. The velocity field distribution of the y-z section of the transformer is shown in Figure 8. The velocity field distribution of the x-z section is shown in Figure 9. The steady-state temperature field distribution is shown in Figure 10.

From Figure 8 and Figure 9, it can be seen that the oil velocity in the upper part of the transformer is greater than that in the lower part, and the high oil velocity is concentrated near the iron core and winding. The reason is that the increase in

TABLE 3. Boundary conditions of thermal field.

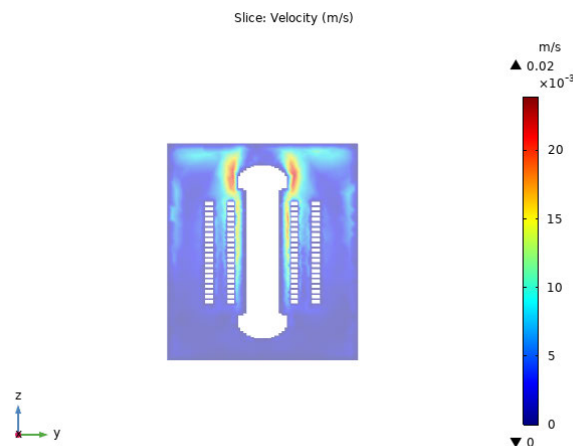| Heat flux	Heat transfer coefficient	External temperature
Convective heat flux	10 W/(m^2·K)	293.15 K

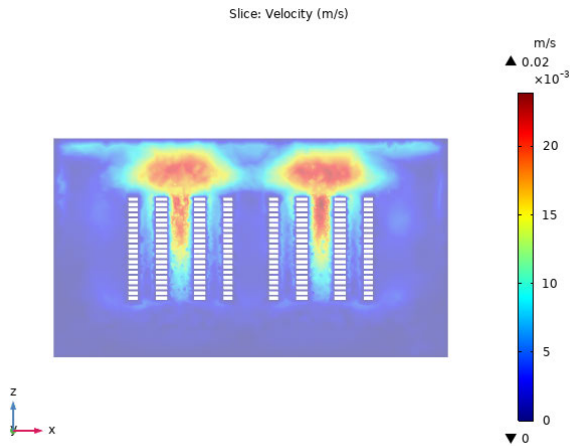**FIGURE 8.** Distribution diagram of velocity field on y-z section of transformer.

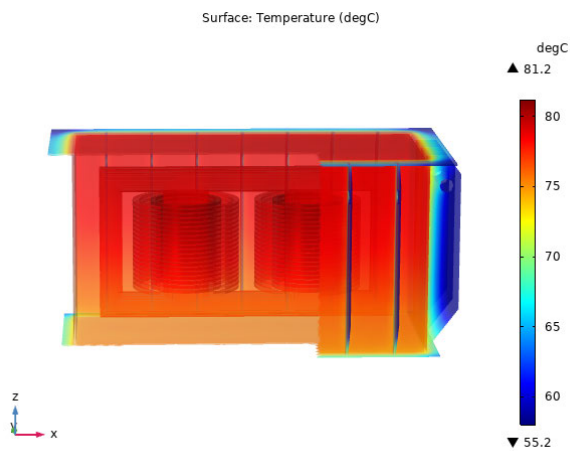**FIGURE 9.** Distribution diagram of velocity field on x-z section of transformer.

FIGURE 10. Overall temperature distribution of transformer.

FIGURE 11. Temperature distribution of iron core of transformer.

FIGURE 12. Temperature distribution of winding of transformer.

temperature leads to a decrease in the density of transformer oil and a decrease in the dynamic viscosity coefficient. High temperature transformer oil rises, and the upper oil velocity increases. From Figure 10, it can be seen that the maximum temperature of the transformer is 81.2°C, which is located in the upper part of the low-voltage winding. Due to the upward fluctuation of transformer oil at high temperature, the internal temperature distribution of the transformer reflects an overall distribution of high temperature above and low temperature below. The temperature field distribution is also symmetrically distributed with the transformer structure. The temperature distribution of the iron core and winding are shown in Figure 11 and Figure 12, respectively. The temperature distribution of the iron core and winding also follows the distribution of high in the upper part and low in the lower part. The temperature difference between the top and bottom is 3.9 °C of the iron core, and 4.2 °C of the winding. The distribution of velocity field and temperature field conforms to the heat transfer principle and is consistent with the actual operating conditions, which verifies the validity of the simulation model.
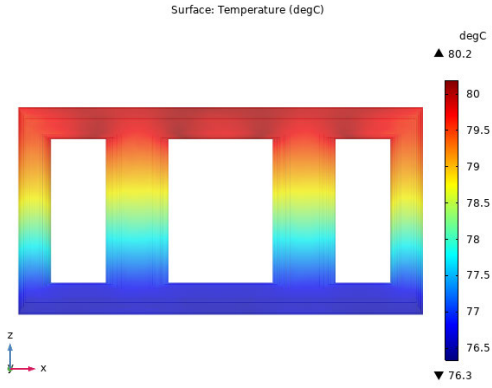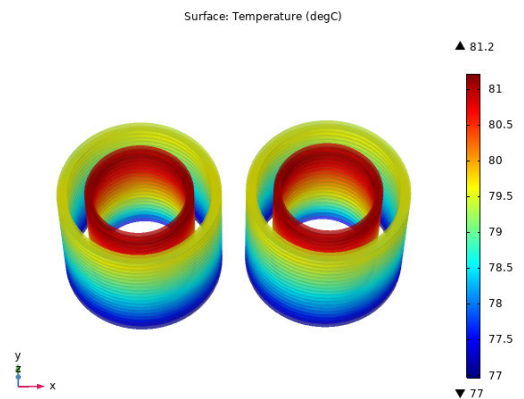
The temperature distribution curve of the windings from bottom to top is shown in Figure 13. It can be seen that the temperature distribution trend of the low-voltage winding and the high-voltage winding is basically the same from the bottom to the top, both gradually increasing with the increase of height, and decreasing slightly below the top. The highest temperature of 81.2 °C occurs below the top of the low-voltage winding.
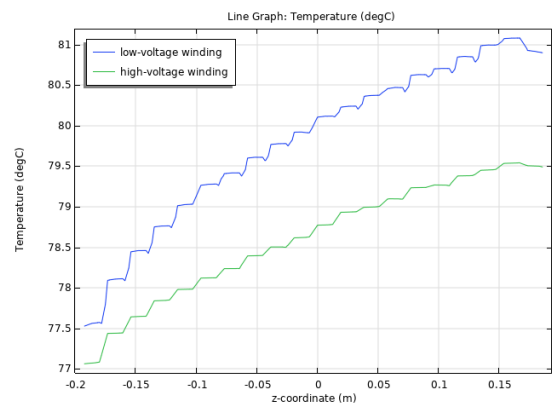

FIGURE 13. Temperature distribution curve of winding.

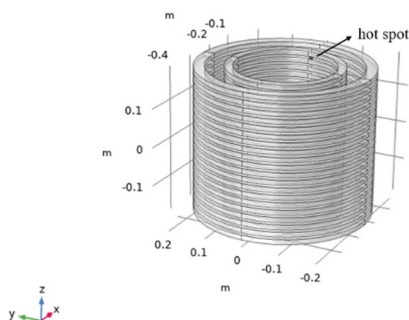The temperature data is exported and processed to obtain coordinates (−0.1225 m, -0.0047 m, 0.1665 m) at

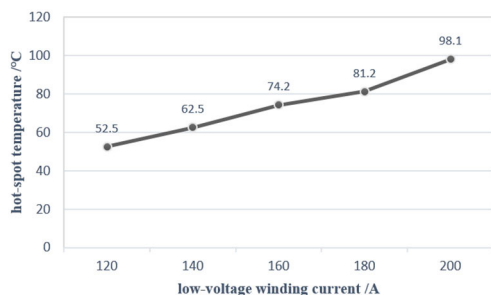**FIGURE 14.** Schematic diagram of the highest temperature point position.

FIGURE 15. The curve of transformer hot-spot temperature changing with low-voltage winding current.

TABLE 4. Coordinates of hot-spots under different currents.

Low-voltage winding current	Hot-spot coordinate
200 A	（-0.2699 m，-0.1399 m，0.1665 m）
180 A	（-0.1225 m，-0.0047 m，0.1665 m）
160 A	（-0.1139 m，0.0041 m，0.1699 m）
140 A	（-0.1139 m，0.0041 m，0.1699 m）
120 A	（0.4006 m，-0.0261 m，0.1699 m）

a temperature of 81.2 °C, as shown in Figure 14. Through calculation, it is known that the highest temperature point is located at 86.49% of the total height of the low-voltage winding.

The above simulation results are obtained at a low-voltage winding current of 180 A and a high-voltage winding current of 70 A. To study the effect of current values on the hot-spot temperature and position of transformer, we apply different current values to the windings and simulate the corresponding hot-spot temperature and position. The curve of transformer hot-spot temperature changing with low-voltage winding current is shown in Figure 15. The coordinates of hot-spots under different currents are shown in table 4.

From Figure 15, it can be seen that as the current increases, the hot-spot temperature increases. When the low-voltage winding current is 200 A, the hot-spot temperature reaches 98.1 °C, which is 16.9 °C higher than the current of 180 A. From Table 4, it can be seen that there is no obvious relationship between the hot-spot coordinate and the current. But the z-coordinates in the hot-spot coordinates of these five sets of simulation data are very close. When the low-voltage winding

current is 200 A and 180 A, the hot-spot is located at the 86.49% of the total height of the low-voltage winding. When the low-voltage winding current is 160 A, 140 A, and 120 A, the hot-spot is located at the 88.26% of the total height of the low-voltage winding. It can be concluded that when the load current changes, the hot-spot fluctuates within the range of 85% - 90% of the total height of the low-voltage winding.

V. CONCLUSION

An oil-immersed transformer is modeled in this paper. A multi-physical field simulation model of magnetic, thermal, and fluid is established using finite element simulation software. By conducting finite element analysis on the simulation model, the magnetic field distribution and losses distribution of the iron core and winding are obtained. The oil flow distribution, 3-D temperature field distribution, and temperature and location distribution of hot-spot are obtained by using the losses as heat source. The simulation of transformer hot-spot temperature and position under different load currents is also conducted. The result shows that when the load current changes, the hot-spot fluctuates within the range of 85% - 90% of the total height of the low-voltage winding. This simulation model and results provide a perspective for monitoring the temperature distribution and hot spot temperature of oil-immersed transformers.

REFERENCES

[1] K. Kierczynski, P. Rogalski, V. Bondariev, P. Okal, and D. Korenciak, "Research on the influence of moisture exchange between oil and cellulose on the electrical parameters of the insulating oil in power transformers," *Energies*, vol. 15, no. 20, p. 7681, Oct. 2022.

[2] M. Zhang, S. Lei, H. Liu, Y. Shen, J. Liu, Y. Shi, H. Jia, and L. Li, "Research on nonlinear characteristics for frequency domain dielectric response of transformer oil-paper insulation," *Measurement*, vol. 204, Nov. 2022, Art. no. 112103.

[3] A. Abdali, A. Abedi, H. Masoumkhani, K. Mazlumi, A. Rabiee, and J. M. Guerrero, "Magnetic-thermal analysis of distribution transformer: Validation via optical fiber sensors and thermography," *Int. J. Electr. Power Energy Syst.*, vol. 153, Nov. 2023, Art. no. 109346.

[4] M. Nicola, C. I. Nicola, D. Sacerdotianu, I. Hurezeanu, and M. Duta, "Monitoring system for power transformer windings hot spot temperature using fiber optic sensors, Kalman filter and integration in SCADA system," *Amer. J. Signal Process.*, vol. 8, no. 2, pp. 33–44, 2018.

[5] Y. Jiang, S. Liu, L. Xiao, and W. Li, "Fiber Bragg grating sensors for temperature monitoring in oil-immersed transformers," in *Proc. 15th Int. Conf. Opt. Commun. Netw. (ICOCN)*, Sep. 2016, pp. 1–3.

[6] C. Chi, F. Yang, C. Xu, L. Cheng, and C. Yang, "A multi-scale thermal-fluid coupling model for ONAN transformer considering entire circulating oil systems," *Int. J. Electr. Power Energy Syst.*, vol. 135, Feb. 2022, Art. no. 107614.

[7] M. Mikhak-Beyranvand, J. Faiz, and B. Rezaeealam, "Thermal analysis of power transformer using an improved dynamic thermal equivalent circuit model," *Electr. Power Compon. Syst.*, vol. 47, no. 18, pp. 1598–1609, Nov. 2019.

[8] L. R. Chandran, G. S. A. Babu, M. G. Nair, and K. Ilango, "A review on status monitoring techniques of transformer and a case study on loss of life calculation of distribution transformers," *Mater. Today, Proc.*, vol. 46, pp. 4659–4666, 2021.

[9] Y. Liu, J. Wang, H. Li, J. Yin, X. Li, and X. Fan, "Temperature field simulation of transformer based on COMSOL multiphysics," in *Proc. IEEE Int. Conf. High Voltage Eng. Appl. (ICHVE)*, Sep. 2020, pp. 1–4.

[10] A. K. Das and S. Chatterjee, "Finite element method-based modelling of flow rate and temperature distribution in an oil-filled disc-type winding transformer using COMSOL multiphysics," *IET Electr. Power Appl.*, vol. 11, no. 4, pp. 664–673, Apr. 2017.

[11] R. Mafra, E. Magalhães, B. Anselmo, F. Belchior, and S. L. E. Silva, "Winding hottest-spot temperature analysis in dry-type transformer using numerical simulation," *Energies*, vol. 12, no. 1, p. 68, Dec. 2018.

[12] S. Khandan, S. Tenbohlen, C. Breuer, and R. Lebreton, "CFD study of fluid flow and temperature distributions in a power transformer winding," in *Proc. IEEE 19th Int. Conf. Dielectric Liquids (ICDL)*, Jun. 2017, pp. 1–4.

[13] R. Guo, J. Lou, Z. Wang, H. Huang, B. Wei, and Y. Zhang, "Simulation and analysis of temperature field of the discrete cooling system transformer based on FLUENT," in *Proc. 1st Int. Conf. Electr. Mater. Power Equip. (ICEMPE)*, May 2017, pp. 287–291.

[14] Y. Jing, Y. Li, X. Yuan, H. Wang, and B. Lu, "Calculation and analysis of the hot-spot temperature-rise for large power transformer based on 3D electromagnetic-fluid-thermal coupling method," in *Proc. 20th Int. Conf. Electr. Mach. Syst. (ICEMS)*, Aug. 2017, pp. 1–4.

[15] L. Li, Y. Zhao, G. Zhu, H. Xiao, X. Liu, H. Chen, W. Jiang, and M. Xue, "Comprehensive thermal analysis of oil-immersed auto-transformer based on multi-physics analyses," *IEEE Trans. Appl. Supercond.*, vol. 31, no. 8, pp. 1–5, Nov. 2021.

[16] J. Li, C. Wei, S. Wang, P. Wu, and Y. Lu, "Multi-physics field simulation of oil-immersed transformers accounting for ambient temperature and load variations," in *Proc. IEEE 6th Int. Electr. Energy Conf. (CIEEC)*, May 2023, pp. 2975–2980.

[17] S. N. E. Dine, X. Mininger, and C. Nore, "Heat transfer in a ferrofluid-based transformer: Multiphysics modeling using the finite element method," *IEEE J. Multiscale Multiphys. Comput. Techn.*, vol. 7, pp. 207–219, 2022.

[18] M. C. Kulan, N. J. Baker, K. A. Liogas, O. Davis, J. Taylor, and A. M. Korsunsky, "Empirical implementation of the steinmetz equation to compute eddy current loss in soft magnetic composite components," *IEEE Access*, vol. 10, pp. 14610–14623, 2022.

[19] Y. You, K. Shao, and Z. Yi, "Dynamic heat dissipation model of distributed parameters for oil-directed and air-forced traction transformers and its experimental validation," *Entropy*, vol. 25, no. 3, p. 457, Mar. 2023.

[20] A. E. Seaver, "An equation for charge decay valid in both conductors and insulators," 2008, *arXiv:0801.4182*.

[21] E. Jiaqiang, B. Luo, D. Han, J. Chen, G. Liao, F. Zhang, and J. Ding, "A comprehensive review on performance improvement of micro energy mechanical system: Heat transfer, micro combustion and energy conversion," *Energy*, vol. 239, Jan. 2022, Art. no. 122509.

[22] X. Yang, Y. Zhao, and S. Cheng, "A multiphysics computational method for thermal field of transformer winding using finite element method," in *Proc. Int. Symp. Insul. Discharge Comput. Power Equip.*, 2023, pp. 635–644.

[23] X. Gou, Z. Huang, and Z. Zhao, "Simulation analysis of spatial electromagnetic field of transformer core considering nonlinear B-H curve," in *Proc. IEEE 3rd Int. Conf. Power, Electron. Comput. Appl. (ICPECA)*, Jan. 2023, pp. 969–976.

[24] Y. Ding, W. Zhang, B. Deng, Y. Gu, Q. Liao, Z. Long, and X. Zhu, "Experimental and numerical investigation on natural convection heat transfer characteristics of vertical 3-D externally finned tubes," *Energy*, vol. 239, Jan. 2022, Art. no. 122050.

[25] S.-I. Takeda, M. Sato, and T. Ogasawara, "Simultaneous measurement of strain and temperature using a tilted fiber Bragg grating," *Sens. Actuators A, Phys.*, vol. 335, Mar. 2022, Art. no. 113346.

XINYAN FENG was born in Jinan, China. He received the master's degree in electrical engineering from Shandong University, Jinan, in 2018.

He is currently a Senior Engineer with State Grid Shandong Electric Extrahigh Voltage Company, primarily engaged in the insulation and fault diagnosis of ultra-high voltage ac/dc equipment.

DA ZHANG was born in Linfen, Shanxi, China. He received the bachelor's degree from North China Electric Power University, Beijing, China, in 2004.

He is currently with State Grid Shandong Electric Extrahigh Voltage Company, focusing on research in live detection and health assessment of substation equipment.

TINGZHI ZHAO was born in Liaocheng, China. He received the master's degree from Huazhong University of Science and Technology, Wuhan, China, in 2014.

He is currently with State Grid Shandong Electric Extrahigh Voltage Company, specializing in live detection and insulation diagnosis of ultra-high voltage ac/dc equipment.

HAN LIU was born in Heze, China. He received the master's degree in high voltage and insulation technology from North China Electric Power University, Beijing, China, in 2017.

He is currently with State Grid Shandong Electric Extrahigh Voltage Company, mainly involved in online monitoring and fault diagnosis of electrical equipment.

YOUFEI SUN was born in Jining, China. He received the master's degree from North China Electric Power University, Beijing, China, in 2016.

He is currently with State Grid Shandong Electric Extrahigh Voltage Company, working on research related to live detection and health assessment of substation equipment.

HAOXIN GUO was born in Yantai, China. He received the B.S. degree from Qingdao University, Qingdao, China, in 2022. He is currently pursuing the master's degree in electrical engineering with Shandong University, Jinan, Shandong, China.

His current research interests include machine learning algorithms for monitoring internal hot spot temperature in converter transformers based on ultrasonic thermometry.

DONGXIN HE received the B.S. degree in electrical engineering from Shandong University, Jinan, China, in 2011, and the Ph.D. degree from North China Electric Power University, Beijing, China, in 2017.

In 2015, he traveled to the LAPLACE Laboratory, University of Toulouse, France, as a Visiting Scholar. He is currently an Associate Professor with Shandong University. He is selected for the Young Talent Lifting Project of China Association for Science and Technology (CAST). His current research interests include space charge characteristics in insulation materials, such as cable insulation and power device encapsulation insulation.

● ● ●